Dual role for B-1a cells in immunity to influenza virus infection

Youn Soo Choi[1,2] and Nicole Baumgarth[1,2,3]

[1]Graduate Group in Immunology, [2]Center for Comparative Medicine, and [3]Department of Pathology, Microbiology and Immunology, School of Veterinary Medicine, University of California, Davis, Davis, CA 95616

B-1 cells are known to contribute most of the "natural antibodies" that are secreted in the steady state, antibodies which are crucial for protection against many pathogens including influenza virus. Whether the CD5$^+$ B-1a subset plays a role during an active immune response is incompletely understood. In contrast to recent data suggesting a passive role for B-1a cells, data provided here show strong highly localized activation of B-1 cells in the draining lymph nodes of the respiratory tract after influenza infection. B-1 cells are identified as a major source for both steady state and infection-induced local virus-neutralizing IgM. The CD5$^+$ B-1a subset is the main B-1 cell subset generating this response. B-1a cell responses are generated by their increased local accumulation rather than by antigen-specific expansion. Our study reveals that during infection with influenza, CD5-expressing B-1a cells respond to and contribute to protection, presumably without the need for B cell receptor–mediated antigen-specific signals, which are known to induce the death of B-1a cells rather than activation. With that, our data reveal fundamental differences in the response regulation of B-1 and B-2 cells during an infection.

CORRESPONDENCE
Nicole Baumgarth:
nbaumgarth@ucdavis.edu

Abbreviations used: AFC, antibody-forming cell; BAL, bronchoalveolar lavage; BCR, B cell receptor; BLF, BAL fluid; GC, germinal center; HI, hemagglutination inhibition; MedLN, mediastinal LN; PerC, peritoneal cavity wash out cell; PLN, peripheral LN.

B-1 cells are a small subset of B cells that secrete most, if not all, natural antibodies in the apparent absence of antigenic challenge. Natural antibodies are often polyreactive and bind to foreign antigens as well as to self-components (1–4). B-1 cell–derived natural antibodies are crucial for host survival from infections. Defects in their production cause increased deaths after infection with bacteria, such as *Salmonella typhimurium* and *Streptococcus pneumoniae* (5–7), and viruses, such as vesicular stomatitis virus, lymphocytic choriomeningitis virus, vaccinia virus, and influenza (2, 8).

B-1 cells are composed of two sister populations, CD5$^+$ B-1a and CD5$^-$ B-1b (9). In addition to their disparate expression of CD5, B-1a and B-1b cells appear also to differ developmentally and functionally (10). Developmental differences between B-1a and B-1b cells were identified by exploiting a hallmark of B-1 cells, namely their ability to self-replenish (11). B-1a and B-1b cell subsets are thought to replenish only themselves and not the other sister population. Although the mechanisms underlying B-1 cells' ability to self-replenish are not understood, earlier studies by Lalor et al. (12) revealed a homeostatic regulatory mechanism by which the presence of normal numbers of B-1 cells in the peritoneal cavity suppresses further B-1 cell expansion and/or de novo development.

The difference in CD5 expression between B-1a and B-1b cells might be a crucial factor determining their in vivo responsiveness to pathogen invasion. CD5 acts as a negative regulator of B cell receptor (BCR)–mediated activation signals (13) and renders B-1a cells nonresponsive to in vitro BCR cross-linking (14). Consistent with the expression of the inhibitor CD5 on B-1a but not B-1b cells, only CD5$^-$ B-1b cells were shown to clonally expand in vivo after infection with *Borrelia hermsii*. After transfer into Rag1$^{-/-}$ mice, B-1b cells rendered recipients protected from *B. hermsii* challenge (15, 16). Although B-1a cells also contributed to immune protection in that system, this was thought to be mediated via natural antibody production. Furthermore, B-1b cells formed strong anti–PPS-3 (pneumococcal polysaccharide-3) immune responses after immunization with either PPS-3 or heat-killed *S. pneumoniae* and conferred immunity against

The Rockefeller University Press $30.00
J. Exp. Med. Vol. 205 No. 13 3053-3064
www.jem.org/cgi/doi/10.1084/jem.20080979

S. pneumoniae after their adoptive transfer into Rag1$^{-/-}$ recipient mice (17). B-1a cells did not mount anti–PPS-3 responses after immunization with heat-killed *S. pneumoniae*. Instead, they secreted high amounts of natural antibodies against phosphocholine, which is another antigenic determinant on *S. pneumoniae* (17). B-1b cells were also shown to mount long-term antibody responses to TI-2 (thymus-independent type-2) antigen, NP-Ficoll (4-hydroxy-3-nitrophenyl-acetyl conjugated to the polysaccharide Ficoll) (18).

Collectively, these data were interpreted as evidence for a mainly passive role for CD5^{+} B-1a cells as producers of natural antibodies and an active role for B-1b cells (19). However, the results from those recent studies are in apparent contrast to earlier studies that had demonstrated an active participation of B-1a cells to *S. pneumoniae* (20, 21). Those earlier studies demonstrated that immunization led B-1a cells to generate the robust and dominant T15 idiotype antibody response to phosphocholine (20, 21), which provides immune protection against reinfection with *S. pneumoniae* (22). Furthermore, although B-1a cells do not respond to BCR-mediated signals they strongly respond to various innate signals both in vivo and in vitro (13, 23).

Natural antibodies produced by B-1 cells are mostly of the IgM isotype (1). Thus, these antibodies can also be transported via the polymeric Ig receptor onto mucosal surfaces and contribute to mucosal immune defenses (24, 25). We previously showed that natural IgM secretion by B-1 cells is required for maximal protection against influenza virus–induced deaths by demonstrating enhanced mortality of mice that lacked B-1 cell–derived IgM but had normal levels of B-2 cell IgM (2, 26). This enhanced mortality after influenza virus infection was partially restored by transfer of natural IgM-containing serum from noninfected WT mice, whereas serum from secretory IgM KO mice (sIgM$^{-/-}$) had no effect. Lung viral titers were significantly higher in influenza virus–infected sIgM$^{-/-}$ mice compared with WT controls (26). Because B-1 cell–derived virus-binding serum IgM levels were unaltered after infection, we concluded in our earlier studies that B-1 cells play a mainly passive role in immune protection to influenza (2), which is consistent with the findings of others (8).

Given the apparent contradictory data on B-1 cells, in particular B-1a cells, regarding their contributions to the active humoral response, we reexamined the responsiveness of B-1 cells to infection with influenza virus in the physiological context of an intact immune system. Collectively our data show strong highly localized activation of B-1 cells in the draining LN of the respiratory tract after influenza infection and identify B-1 cells as a major source for local virus-neutralizing IgM. The CD5^{+} B-1a subset was the main B-1 cell subset generating this response. The response was generated by increased local accumulation of B-1a cells, but not B-1b cells, rather than by antigen-specific expansion. Our study thus reveals that during infection with influenza, CD5-expressing B-1a cells respond to and contribute to protection, presumably without the need for BCR-mediated antigen-specific signals, which are known to induce death of B-1a cells rather than activation. With that, our data also reveal fundamental differences in the response regulation of B-1 and B-2 cells during an infection.

RESULTS

We previously showed that B-1 cells importantly contribute to protection from influenza virus infection via secretion of IgM (2, 26). Consistent with our findings, others recently showed a requirement for BLIMP-1 (B lymphocyte–induced maturation protein 1)–dependent differentiation to antibody-secreting cells for B-1 cell–mediated protection from influenza infection (27). The protective effects of B-1 cells did not appear to require infection-induced enhanced B-1 cell–derived IgM secretion, as serum IgM levels were unchanged after infection and passive transfer of serum from noninfected WT mice at least partially restored protection (26). However, typical influenza virus infection is highly restricted to the respiratory tract and protection might be mediated by local immune defense mechanisms. Because IgM can be transported onto the mucosal surface of the respiratory tract (24, 25), we aimed to study the potential contributions of B-1 cells to the local immune responses against influenza virus.

A challenge for studies on B-1 cells in the physiological context of an intact host is the lack of a specific marker that distinguishes all B-1 cells from conventional (B-2) cells. To overcome this hurdle, we generated Ig allotype chimeras by neonatal allotype-specific anti-IgM treatment and adoptive transfer of allotype-disparate congenic peritoneal cavity wash-out cells (PerC) according to previously published protocols (2, 12). After full reconstitution, these mice contain B-1 and B-2 cells of disparate allotypes (Igh-a and Igh-b, respectively for the studies in this paper) as described in detail elsewhere (2). B-1 and B-2 cells and the antibodies they produce are distinguished using Ig allotype and isotype-specific monoclonal antibodies. As shown earlier, in these chimeras all donor-derived Igh-a is of B-1 cell origin and 80–90% of the host Igh-b is B-2 cell derived (2). For easier reading of the text we will refer to donor and host-derived Ig as B-1 and B-2 cell derived, respectively.

B-1 cells produce natural IgM in the respiratory tract

Using these mice we confirmed our previous findings that most of the serum natural IgM was Igh-a (87 ± 3.4%; Fig. 1 A) and thus was produced by B-1 cells. We also detected steady state–secreted natural IgM in the bronchoalveolar lavage (BAL). Somewhat surprisingly, B-1 cells provided >99% of natural influenza-binding IgM in the airway space (88 ± 14 U/mg for B-1 and 0.4 ± 0.01 U/mg for B-2; Fig. 1 B). Given that small amounts of natural influenza-binding IgM might be produced by host-derived B-1 cells (2), it is likely that all respiratory tract IgM in the steady state is B-1 cell derived. Consistent with this, B-1 cells generated >90% of the natural total and virus-specific IgM-secreting antibody-forming cells (AFCs) in lung tissue as measured by ELISPOT (Fig. 1 C). Overall, IgM secretion in the chimeras was comparable to that of BALB/c mice, indicating that allotype chimera

have normal levels of local natural IgM (Fig. 1). The slightly higher expression in the chimeras is likely because of the different ages used for comparison (8–10 wk and >4 mo for BALB/c mice and chimeras, respectively) and does not reflect differences caused by the generation of the chimeras. The data confirm and extend previous studies on the importance of B-1 cells as producers of much of the steady state IgM produced systemically in serum (2, 26) as well locally in the respiratory tract as shown here.

Induction of local B-1 cell responses after influenza virus infection

Although B-1 cells contribute most of the preinfection influenza-binding serum IgM, the enhanced systemic production of serum IgM after infection with this virus is exclusively B-2 cell derived (2). We evaluated the contributions of B-1 and B-2 cells to local respiratory tract IgM production after infection by conducting allotypes-specific ELISA with BAL and serum from two litters of allotype chimeras. One litter was studied at days 0, 5, and 7 after infection and the other at days 7 and 10. Confirming our previous studies, neither systemic virus-specific (Fig. 2 A) nor total (not depicted) B-1 cell–derived IgM titers were altered in the serum after infection, whereas B-2 cell–derived IgM was strongly induced (Fig. 2 A). In stark contrast to the systemic response, local B-1 cell–derived influenza-binding IgM was strongly increased in the BAL during the course of infection, whereas B-2 cell–derived IgM was only weakly induced (Fig. 2 B). Local IgM responses in WT BALB/c mice showed similar kinetics to the allotype chimeras (Fig. 2 B). These results show a remarkable dichotomy in the response of B-1 cells to infection with influenza virus.

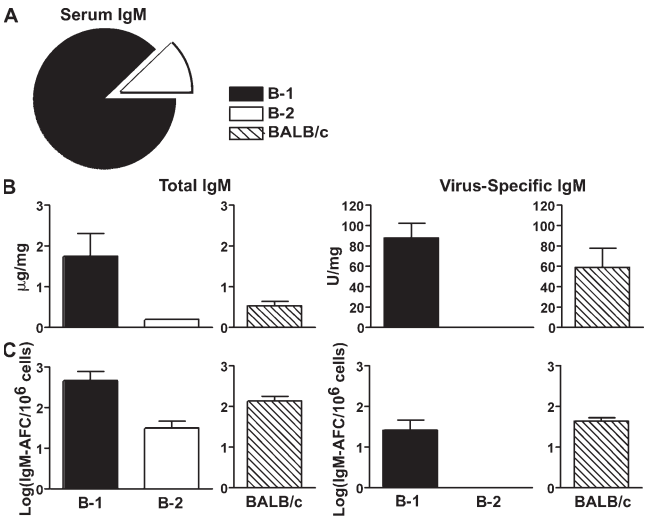

Figure 1. B-1 cells are major producers of natural IgM in serum and airways. (A) Shown are relative amounts of B-1 and B-2 cell–derived total serum IgM in noninfected Ig allotype chimeras ($n = 5$) measured by ELISA. As shown previously (2), B-1 cells (Igh-a) are the main source of serum IgM (black; 87 ± 3.4% of total IgM). (B) Shown are mean concentrations ± SD of total (left) and virus IgM (right) per milligrams of total protein, derived from B-1 (Igh-a; black) and B-2 (Igh-b; white) cells in the BLF of chimeras ($n = 2$). Data for BALB/c mice ($n = 4$; hatched bars) are shown for comparison. (C) Shown are the mean frequencies ± SD of total (left) and virus-specific (right) IgM-secreting cells in the lung tissue of the same chimeras and control BALB/c mice. Data are from one of three experiments done with chimeras that yielded comparable results.

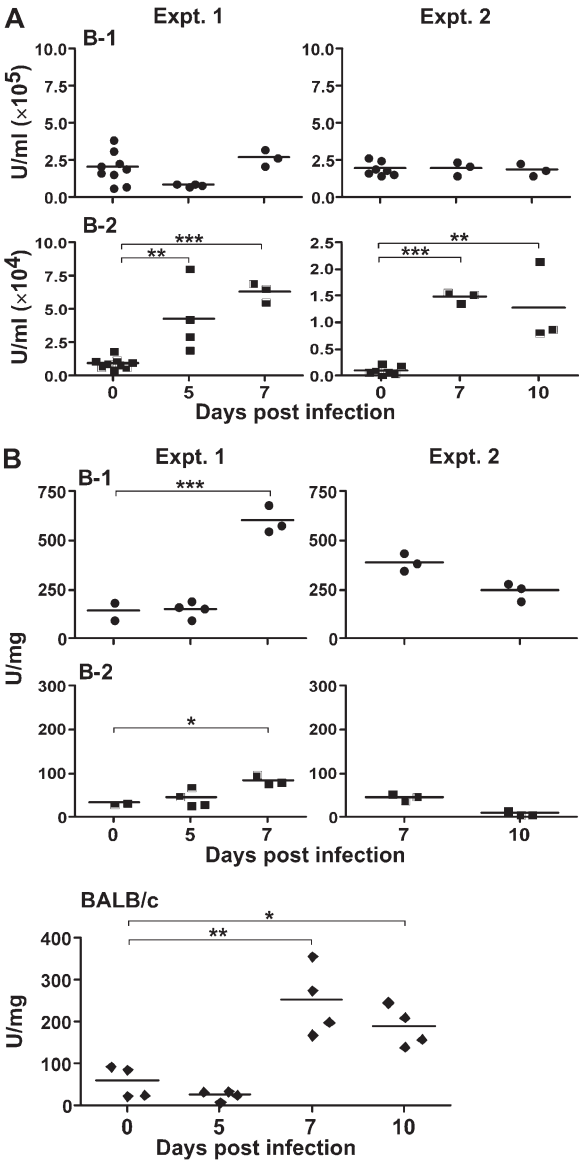

Figure 2. B-1 cells respond to influenza infection locally but not systemically with increased IgM production. Shown are serum (A) and BLF (B) IgM levels from individual Ig allotype chimeras and BALB/c mice, respectively, at indicated times after influenza A/Mem/71 infection. Two groups of mice were analyzed (experiment (Expt.) 1 and experiment 2, $n =$ 2–4 mice per time point). B-1 (A and B, circles) and B-2 (A and B, squares) cell–derived virus-specific IgM levels (in units per milliliter) were determined in chimeras by allotypes-specific IgM ELISA. IgM concentrations in BLF were normalized to total protein concentrations (in units per milligram). BLF data for BALB/c mice (B, diamonds) are shown for comparison. Results represent one of two sets of experiments done that yielded comparable results. Statistical analysis was conducted using ONE-way ANOVA (Tukey's multiple comparison test: *, $P < 0.05$; **, $P < 0.01$; ***, $P < 0.001$).

Although systemic natural IgM levels are maintained at the steady state, B-1 cells respond strongly with increased IgM secretion in a tissue-restricted manner at the site of infection.

Antiviral activity of locally secreted IgM

To determine the functional significance of local B-1 cell IgM secretion, we studied the antiviral properties of IgM in the BAL fluid (BLF) using a chicken RBC hemagglutination inhibition (HI) assay. We could use BLF from BALB/c mice instead of having to generate chimeras because >99% of preinfection influenza-binding IgM is produced by B-1 cells (Fig. 1 B). We compared HI activity in BLF taken at days 0 and 7 of infection, both before and after removal of IgM via affinity chromatography. ELISA analysis confirmed the successful removal of virus IgM in these samples (Fig. 3 A). The removal of IgM reduced the antiviral HI activity by >75% when BLF was received from noninfected mice and to ∼50% when BLF was taken on day 7 of infection (Fig. 3 B). The smaller contributions of IgM in BLF from infected mice are explained by the increases in virus-specific antibodies of other isotypes (Fig. 3 C). Thus, B-1 cell–derived IgM has relevant functional antiviral activity. Furthermore, the data suggest that B-1 cells provide immune protection to influenza virus by two distinct mechanisms: the generation of steady-state systemic and local natural antibodies and the rapid local induction of antiviral IgM by actively participating in local humoral response to influenza virus infection. This provides an explanation for why transfer of natural IgM only in part reconstituted protection from influenza-induced death in mice that lacked IgM-secreting B-1 cells (26).

Effector B-1 cells accumulate in the mediastinal LN (MedLN) after influenza virus infection

To determine the site of B-1 cell–induced IgM secretion after influenza virus infection, we performed ELISPOT analysis on regional MedLN as well as on spleen and lung tissue. Because MedLN are not visible in noninfected mice, we compared frequencies of infection-induced IgM secretors with those found in nonstimulated peripheral LN (PLN). Influenza IgM-secreting B-1 cells (effector B-1 cells) accumulated in MedLN within 5 d of infection, which is comparable to the responses by B-2 cells (Fig. 4 A). Influenza IgM-secreting B-1 cells were not found in PLN (unpublished data). BALB/c mice showed a similar accumulation of influenza IgM-secreting AFCs in MedLN although somewhat faster kinetics of the response (Fig. 4 B). In the spleen, effector B-1 cells were found to comparable frequencies before and after infection (Fig. 4 C), which is consistent with the unchanged levels of B-1 cell–derived serum IgM (Fig. 2 A). Interestingly, the frequencies of virus-specific IgM AFCs were consistently reduced in the lung tissue of BALB/c mice and chimeras after infection (unpublished data), suggesting that the BAL IgM is not produced solely by cells residing in the lung.

To determine the phenotype of the B cell subset that generated the local IgM response to influenza virus infection, we conducted IgM ELISPOT analysis on FACS-purified MedLN B cells from BALB/c mice, which were separated into four subsets according to expressions of surface IgM and CD43 (Fig. 4 D). The IgM^+CD43^+ B cell population was the only significant source of IgM-secreting cells (Fig. 4 D). They expressed the same phenotype as the B-1 cells identified in the allotype chimeras (see following paragraph), namely $FS\text{-}C^{hi}$ $CD19^{hi}$ IgM^{hi} IgD^{lo} $CD43^+$ (Fig. 4 and not depicted).

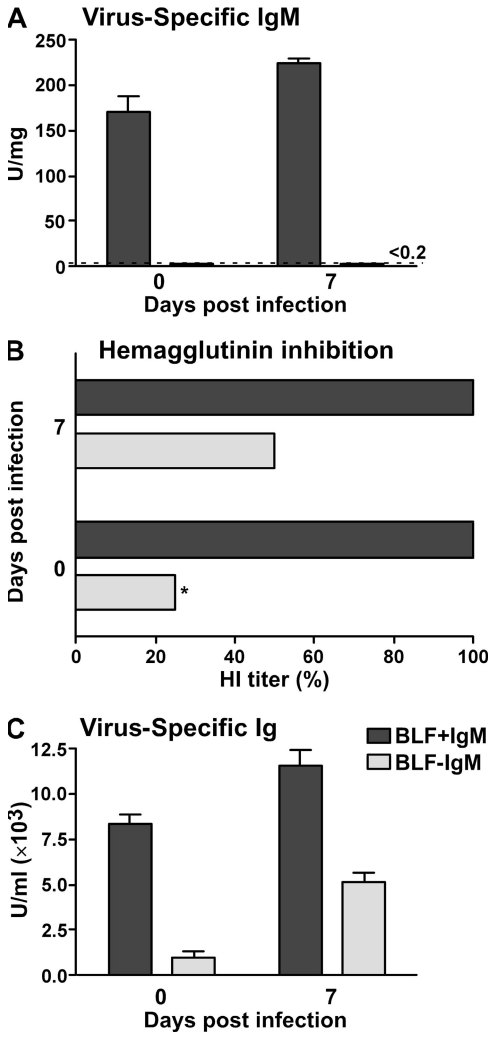

Figure 3. IgM is a major virus-neutralizing activity in BLF of noninfected and infected mice. BLFs from noninfected and day-7 infected BALB/c mice (n = 12 per time point) were pooled and analyzed for HI activity before and after depletion of IgM by affinity chromatography. (A) ELISA analysis, performed for each sample in triplicate, confirmed the presence of virus IgM in the unfractionated BLF and then the complete removal of virus IgM by this procedure. Data shown are the mean ± SD relative concentrations (in units per milligram of total protein) of virus-specific IgM in BLF samples before (dark gray) and after (light gray) IgM depletion. (B) Shown are relative decreases (in percentage) in HI titers of BLF after removal of IgM (light gray) compared with the complete BLF samples before IgM was removed (dark gray). *, HI activity of total BLF from noninfected mice was not titrated out fully. Relative decrease of HI titer after IgM depletion was at least 75%. Results are from one representative sample of triplicates in all assays. (C) Mean ± SD relative units of influenza-binding total Ig (in units per milliliter of BLF), i.e., virus IgM, IgG, and IgA, were determined in triplicate BLF samples before and after IgM depletion (dark gray and light gray, respectively) by ELISA.

FACS analysis of MedLN from day-7 infected mice with allotypes-specific anti-IgMa and -IgDa revealed the presence of B-1 cells (~1% of $CD19^+$ cells), which expressed surface Ig at levels comparable to that of peritoneal cavity B-1 cells (Fig. 5 A). Frequencies of B-1 cells were also determined in spleen and PLN (Fig. 5 B). Consistent with the ELISPOT data (Fig. 4), increased frequencies of B-1 cells after influenza infection were seen only in MedLN but not PLN or spleen (Fig. 5 B). Donor-derived B-1 ($IgMa^+$ $IgDa^+$) cells were larger in size and expressed higher levels of CD19 than host-derived B-2 cells. In addition, they expressed CD43 consistent with the known phenotype of B-1 cells (Fig. 5 C) (28, 29). Consistent with studies by others (30), CD138, a marker of differentiated plasma cells, was not expressed to significant levels on MedLN B-1 cells (Fig. 4 C) despite their ability to secrete IgM (Fig. 4). Together, these results demonstrate that IgM^{hi} IgD^{lo} $CD19^+$ $CD24^{interm}$ $CD38^{hi}$ $CD43^+$ $CD138^-$ and $CD5^+$ or $CD5^-$ B-1 cells actively participate in the local immune response to influenza virus infection by accumulating in the draining LN at the site of infection, but not in infected tissues, and by differentiating to IgM^+ antibody-secreting cells that lack signs of terminal differentiation.

Local B-1 cell responses lack signs of antigen-specific activation

Respiratory tract B-1 cell responses were measurable by day 5 of infection and peaked around day 7 (Fig. 4 A). B-1 cells were not found among the $CD24^{hi}CD38^{lo}$ (28, 31) germinal center

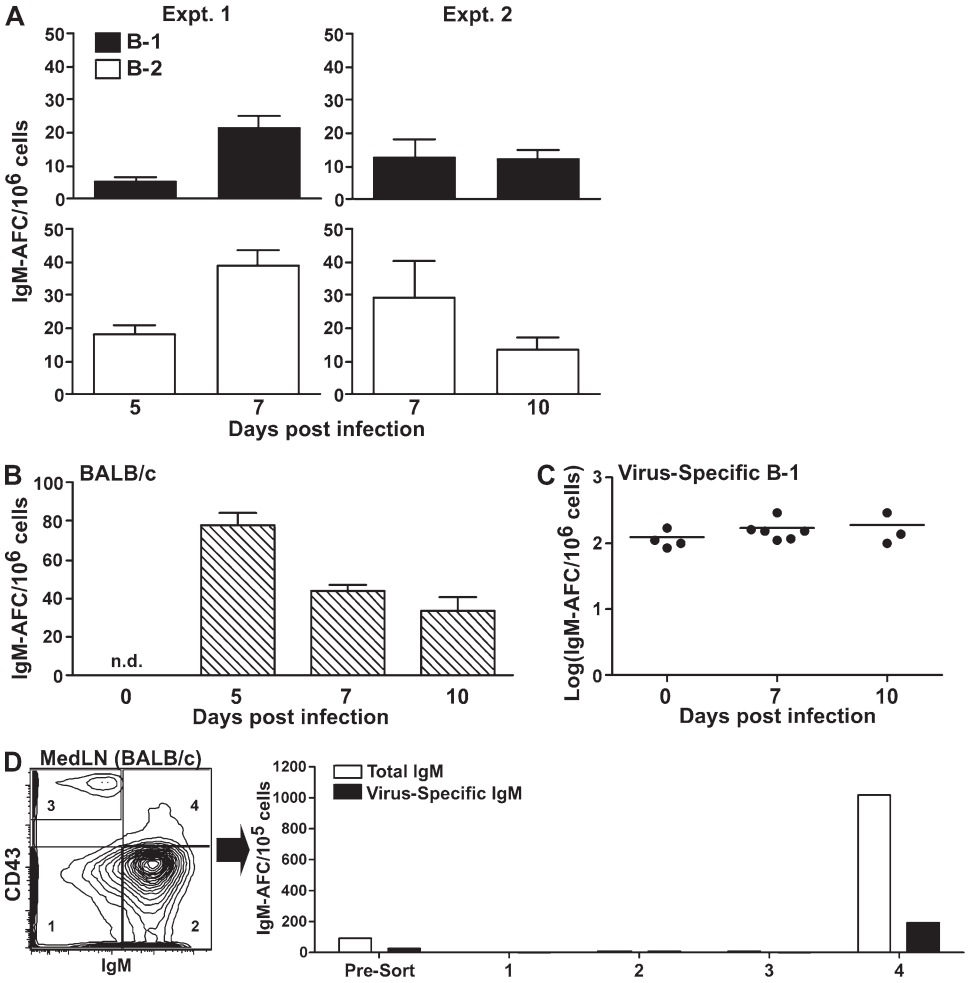

Figure 4. Infection-induced accumulation of IgM-secreting B-1 cells in local LN. (A) Shown are the mean frequencies ± SD of virus-specific IgM-secreting B-1 (Igh-a) and B-2 (Igh-b) cells in MedLN after infection of Ig allotype chimeras with A/Mem/71 (n = 3 and 4, respectively, per time point). Results are from two independent ELISPOT analyses conducted on days 5 and 7 (experiment (Expt.) 1, left) and 7 and 10 (experiment 2, right), after infection. Results represent one of two sets of experiments done that yielded comparable results. (B) Virus-specific IgM-secreting B cells were enumerated in the MedLN of BALB/c mice (n = 4 per time point) for comparison. Shown are the mean frequencies ± SD of virus-specific IgM-secreting cells. n.d., not detectable by eye. (C) Frequencies of influenza virus–specific IgM-secreting B-1 cells in the spleens of individual chimeras assessed by ELISPOT at the indicated times after infection. Data are from one of two independent experiments that yielded similar results. Bars show the means. (D) Shown is a 5% contour plot (left) of $CD19^+$ B cells from MedLN of day-7 infected BALB/c mice after exclusion of dead cells and T cells (CD4 and 8). Cells were sorted as indicated into four populations based on IgM and CD43 expression. Total and virus-specific IgM-secreting B cells were enumerated for each subset by ELISPOT.

(GC) B cells that develop and expand in the MedLN around day 6/7 after infection (Fig. 6 A). More than 20% of GC B cells expressed host-derived IgMb. The others were surface IgM and IgD negative (unpublished data) and, thus, we would have expected to identify IgMa$^+$ GC B cells had they been induced.

To determine whether there was evidence for extrafollicular clonal expansion of virus-specific IgM-secreting effector B-1 cells in MedLN, i.e., whether the B-1 cell response showed signs of antigen specificity, we compared the frequencies of virus-specific effector B-1 cells over total IgM-secreting B-1 cells at days 7 and 10 of infection. On both days studied, the virus-specific effector B-1 cells made ~10% of the total B-1 cells that accumulated in the MedLN after infection (Fig. 6 B). Thus, we found no evidence for a preferential expansion of virus-specific B-1 cells in MedLN. Similar frequencies of virus IgM–secreting B-1 cells were also observed in the spleen of mice before and after infection, further suggesting that the infection does not cause an expansion of virus-binding B-1 cells and that any increased secretion of B-1 cell–derived IgM was the consequence of infection-induced immune signals rather than a response to a particular viral antigen.

To determine whether the observed increases in MedLN B-1 cells after infection were caused by recruitment or clonal expansion of these cells, we studied the rate of BrdU incorporation within the individual B cell subsets of MedLN from 7-d infected mice. The mice received BrdU via injection and drinking water for 24 h before tissue harvest. Frequencies of BrdU$^+$ cells within each B cell compartment were compared with those in PLN of sham-infected controls (Fig. 6 C). Data are expressed as fold differences in BrdU incorporation between LN B cell subsets in infected and sham-infected mice. The data revealed the strong infection-induced proliferation among conventional B cell subsets in MedLN, particularly the IgM$^-$ CD43^{hi} plasmablasts (Fig. 6 C). In striking contrast, there was a complete lack of influenza infection–induced increases in B-1 (IgM^{hi}IgD^{lo}CD19^{hi}CD43$^+$) cell proliferation in MedLN, implying that these cells do not undergo significant antigen-driven expansion at the site. All splenic B cell subsets from the same mice lacked signs of proliferation beyond those found in sham-infected controls (Fig. 6 C), underscoring the tissue-specific nature of the humoral response at this time point. Consistent with a lack of local expansion, B-1 cells in MedLN and in the (nonresponding) spleen had similar forward scatter/side scatter profiles, further suggesting that MedLN B-1 cells did not undergo blast transformation (Fig. 6 D).

Importantly, the majority of B-1 cells (>70%) in the MedLN expressed the BCR-signaling inhibitor CD5 and thus were B-1a cells (Fig. 6 D). Together, these results show that the highly localized B-1 cell response to influenza virus infection is facilitated by the increased accumulation, not expansion, of B-1a cells in the regional LN at the site of infection.

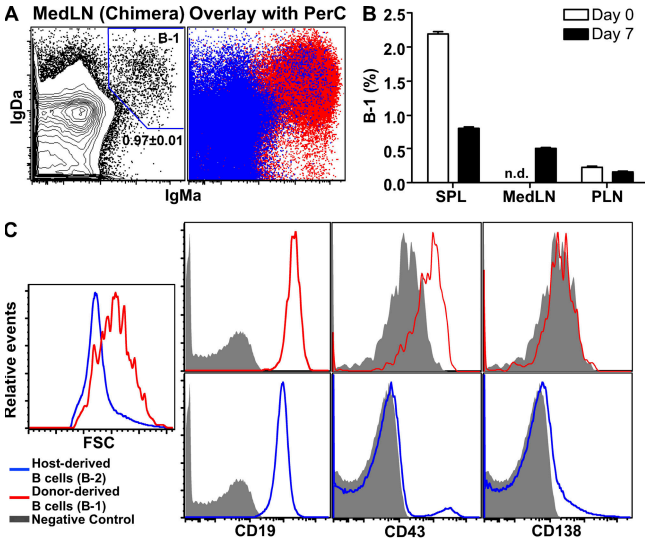

Figure 5. Characterization of B-1 cells in MedLN after influenza virus infection. (A) Shown is a 5% contour plot with outliers (left) of live CD19$^+$ B cells from day-7 influenza-infected Ig allotype chimeras after exclusion of dead cells, T cells (CD3, 4, and 8), macrophages (F4/80), NK cells (DX-5), and granulocytes (GR-1). B-1 cells in MedLN were identified by their expressions of IgMa and IgDa. Overlay dot plot (right) of MedLN B-1 cells (blue dots) with similarly gated CD19$^+$ B cells from the peritoneal cavity (PerC, red dots) showed their similar phenotype. (B) Shown are the mean frequencies ± SD of IgMa$^+$ IgDa$^+$ B-1 cells in spleen (SPL), MedLN, and PLN of chimeras on days 0 and 7 after infection. n.d., not detectable by eye. (C) Shown are histogram overlay diagrams for forward side scatter (FSC) and indicated cell surface markers on IgMa$^+$IgDa$^+$ B-1 cells (red lines) and IgMa$^-$IgDa$^-$ host B-2 cells (blue lines) with negative control staining (gray-filled histogram), gated as outlined for A. Results shown are representative of two experiments that yielded similar results.

B-1a cells actively participate in the local immune response to influenza virus infection

Our findings of an active response by B-1a cells are in apparent contrast to recent studies that suggested a mainly passive role for B-1a cells as steady-state natural antibody producers during systemic bacterial infections (17). To compare the ability of B-1a and B-1b cells to respond to influenza virus infection, we generated irradiation Ig allotype chimeras with either FACS-purified peritoneal cavity B-1a or B-1b cells, or total PerC as controls (Fig. 7 A). Successful reconstitution of the animals was confirmed by serum ELISA. Overall serum IgM levels in these reconstituted animals were lower than in neonatal antibody-treated chimeras or normal mice (unpublished data); however, this is likely because of the relative smaller number of transferred B-1 cells.

The small frequency of B-1a and B-1b cells that was co-transferred with the purified B-1 cell subset of interest seemed to have homeostatically expanded during the 6-wk reconstitution phase (compare purities of the input cells [Fig. 7 A] with the peritoneal cavity B-1 cell subset frequencies for each group [Fig. 7 B, top left]). Nonetheless, a relative enrichment of the transferred FACS-purified B-1 subset remained in the recipient mice compared with mice receiving total washouts (Fig. 7 B, PerC). Analysis on day 7 after infection with influenza showed that mice that received purified B-1a cells showed similar overall frequencies of B-1a and B-1b cells in all of the studied tissues compared with those that received

total PerC. This included the respiratory tract draining MedLN, in which ~80% of the B-1 cells were B-1a. In contrast, mice that received purified B-1b had increased frequencies of B-1b over B-1a cells in PerC, PLN, and spleen. In the MedLN, however, these mice had more B-1a than B-1b cells. Thus, in all mice, independent of the type of B-1 cells they received, B-1 cells that accumulated in the MedLN were mostly of the B-1a subset (Fig. 7 B). Even in B-1b recipients, in which ~25% of the B-1 cells in the PerC were B-1a, ~65% of the B-1 cells in MedLN were B-1a cells. Moreover, although total B-1 cell numbers in MedLN were overall similar in recipients of total PerC and B-1a cells (4,723 ± 1,512 and 3,623 ± 1,469; $n = 4$), B-1 cell recovery from the MedLN of B-1b recipients was ~20-fold lower (262 ± 80; $n = 4$), thus showing little recruitment of B-1 cells to the side of infection in mice that lack B-1a cells.

IgM-secreting B-1 (Igh-a) cells were found in each group of recipients (Fig. 7 C). B-1b cell recipients had the smallest number of IgM-secreting B-1 cells. This further demonstrates that B-1a cells not only accumulate in the MedLN but also contribute the majority of the locally secreted IgM. Consistent with studies in neonatal chimeras (Fig. 6), roughly 5–10% of these IgM-secreting cells were influenza-binding IgM (Fig. 7 C). Collectively, these results demonstrate the rapid activation of B-1a cells after influenza virus infection and their local accumulation and differentiation to IgM-secreting cells in the regional LN draining the site of infection.

DISCUSSION

We previously showed that B-1 and B-2 cell–derived IgM are nonredundant components of the protective response to acute influenza virus infection (26). B-1 cell–derived immunity appeared to be provided via secretion of steady-state levels of natural serum IgM levels that were unaffected by influenza virus infection. Extending our initial findings, we now provide evidence for an additional active role of B-1 cells, namely as providers of enhanced local (but not systemic) IgM at the site of infection. Importantly, we show that B-1a cells are the main B-1 cell subset contributing to the response, despite their expression of the BCR inhibitor CD5. This conundrum is explained by our findings that B-1a cell responses are tissue restricted and not driven by antigen-specific clonal expansion. Instead, they appear to be regulated by infection-induced local inflammatory signals that cause B-1a cell accumulation and, potentially, B-1a cell differentiation. Thus, our data show that B-1a cells, which undergo apoptosis rather than activation after BCR cross-linking (13), can nonetheless actively contribute to immune defenses against pathogens.

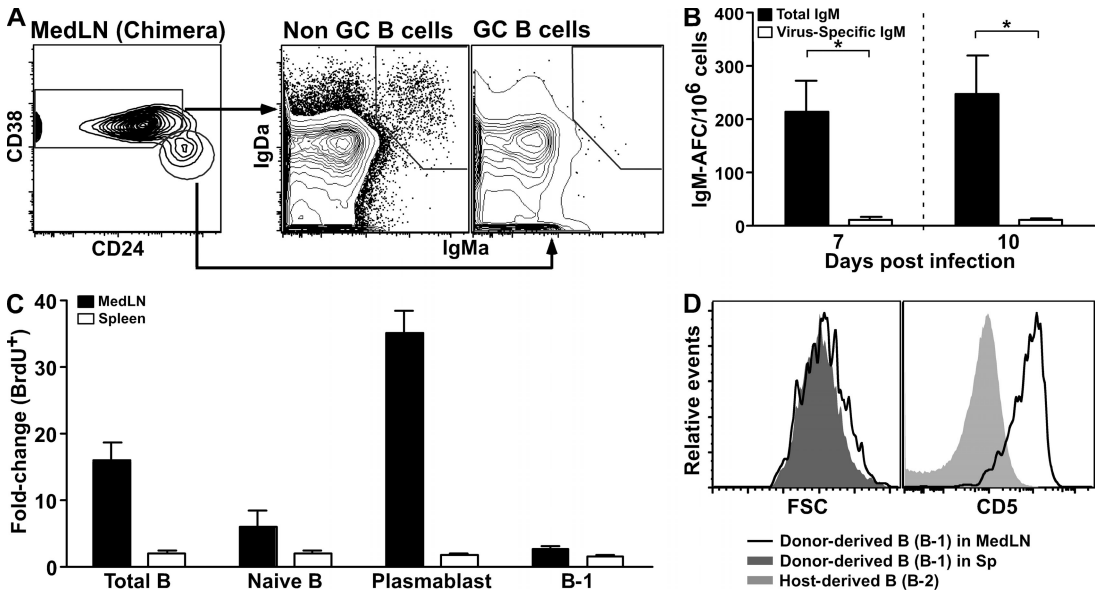

Figure 6. Local B-1 cell response to influenza virus is not antigen driven. Groups of Ig allotype chimeras ($n = 2$ or 3 per time point) were infected with influenza A/Mem/71. (A, left) A 5% contour plot of live CD19$^+$ B cells in MedLN from day-7 infected mice after exclusion of dead cells (propidium iodide$^+$) and/or antibodies against markers for T cells (CD3, 4, and 8), macrophages (F4/80), NK cells (DX-5), and granulocytes (GR-1). GC and non-GC B cells were identified based on their expression of CD24 and CD38. (A, right) The presence of IgMa$^+$IgDa$^+$ B-1 cells is revealed only in the non-GC fraction. (B) Shown are mean frequencies ± SD of total and virus-specific IgM-secreting B-1 (Igh-a) cells in MedLN at the indicated days after influenza infection. Results are representative of two flow cytometry experiments and four ELISPOT analyses. Statistical significance was assessed by a two-tailed Student's *t* test (*, $P < 0.05$). (C) Two groups of BALB/c mice ($n = 4$ per group) were either infected with influenza A/Mem/71 or sham infected for 7 d. BrdU was given 24 h before analysis. Shown are fold differences in frequencies of BrdU$^+$ cells for each indicated B cell subset between influenza infected and sham-infected mice. B cells were identified as total B (CD19$^+$), naive B (IgM^{lo}IgD^{hi}CD43$^-$), plasma (IgM$^-$CD43^{hi}), and B-1 (IgM^{hi}gD^{lo}CD19^{hi}CD43$^+$) cells in MedLN and spleens. Error bars show SD. (D) Shown are overlay histograms for forward side scatter (left) and expression of CD5 (right) on B-1 cells in MedLN (black line) compared with B-1 cells in spleen (dark gray–filled histogram, left) and host B-2 cells (light gray–filled histogram, right). Cells were gated as in Fig. 5 A. Results are from one of four experiments that yielded comparable results.

Recent efforts by us and others have focused on elucidating the extent of B-1 cell responses to various pathogens in vivo (15–17, 23, 26, 32). These studies were precipitated by a large number of earlier studies, which clearly showed that B-1 cell responses differ in many ways from responses by conventional (B-2) cells. Importantly, although B-2 cells are activated to proliferate, migrate, and differentiate to antibody-secreting cells after BCR engagement, B-1 cells do not. Instead, they proliferate vigorously to mitogenic signals such as LPS and respond to PMA in the absence of additional stimulation via calcium ionophores (13, 14). In addition, B-1 cell migration appears to be regulated, at least in part, by an innate immune signal provided via Toll-like receptors. In response to i.p. injection of bacteria or bacterial components such as lipid A and peptidoglycan, B-1 cell migration from the peritoneal cavity was partially dependent on the expression of TLR-4 (32). Yang et al. (23) also showed that B-1a cells migrate from the peritoneal cavity to the spleen after stimulation with LPS, where they proliferate and differentiate into IgM-secreting plasma cells. Collectively, these data indicate that B-1 cells vigorously respond to innate, but not antigen-specific, signals.

The lack of BCR-mediated activation is explained by the expression of CD5 on the majority of B-1 cells. CD5 functions as negative regulator of TCR-mediated activation signals (33), and studies in $CD5^{-/-}$ mice indicate a similar function on B-1a cells (13). Induction of CD5 expression on B-1a cells might follow their positive selection on self-antigens (10) at a particular stage during their development. Up-regulation of CD5 on B cells is also a hallmark of anergic B-2 cells (34). Similar to anergic B-2 cells, CD5 expression on B-1a cells

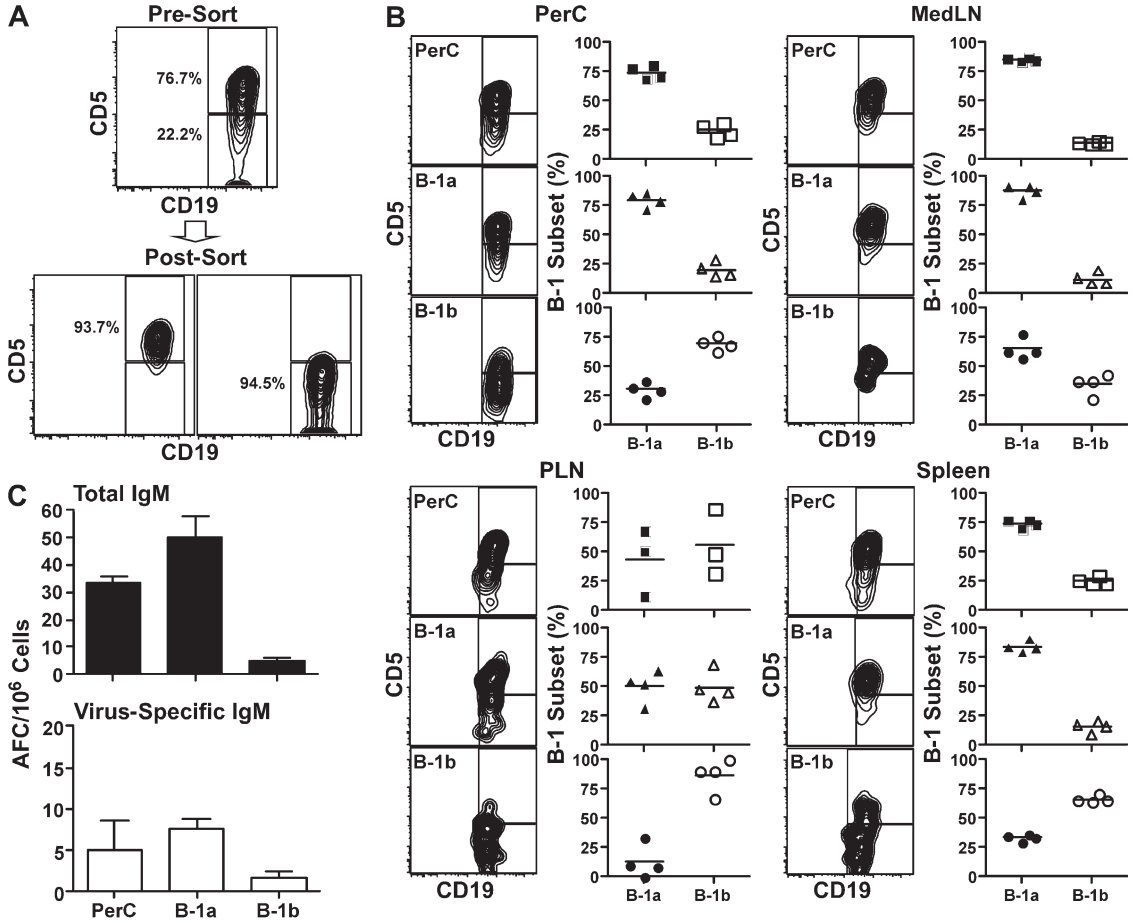

Figure 7. B-1a cells are the major contributors of the IgM responses in regional LN after influenza virus infection. PerC cells from 24 BALB/c mice (Igh-a) were pooled and sorted into B-1a and B-1b by FACS. Total PerC and sorted B-1 cell subsets were transferred together with C.B.-17 BM cells into whole body–irradiated donor C.B.-17 (Igh-b) mice. (A) Shown are 5% contour plots with outliers of PerC cells before (top) and after (bottom) FACS purification into $CD5^+$ (B-1a) and $CD5^-$ (B-1b) $CD11b^+$ $CD19^+$ $CD23^-$ live PerC B-1 cells (not depicted). (B) Shown are results from the FACS analysis of indicated tissues from individual recipient chimeric mice after full reconstitution and infection with influenza virus for 7 d. Contour plots are from one representative example of each group of mice ($n = 4$). Scatter plot indicates the relative frequencies of $CD5^+$ (B-1a; filled symbols) and $CD5^-$ (B-1b; open symbols) cells among $CD19^{hi}CD43^+IgMa^+$ cells in PerC (top left), MedLN (top right), PLN (bottom left), and spleen (bottom right) of recipient mice that had received either total PerC, B-1a, or B-1b cells. Each symbol represents the data from an individual animal and the bar indicates mean of the group. (C) Shown are the mean frequencies ± SD of total and virus-specific IgM-secreting B-1 cells (Igh-a) in MedLN as assessed by ELISPOT with pooled samples from three to four mice per group and analyzed in triplicate.

might function to inhibit their potential inappropriate activation in response to BCR ligation mediated by autoantigen.

Despite the inhibitory function of CD5, >70% of the B-1 cells that accumulated in the regional LN in response to influenza virus infection expressed CD5 (Fig. 6), suggesting that most of the local B-1 cell responses were not driven by BCR-mediated signals. Consistent with this, these locally accumulating B-1 cells showed no signs of antigen-specific expansion. Instead, the virus-specific B-1 cells were recruited into the inflamed MedLN, but no other tissue, always in proportion to their relative frequencies in other tissues and at frequencies similar to those observed before infection (~10% of total IgM-secreting B-1 cells; Fig. 6). Both virus-specific and -nonspecific B-1 cells migrated and/or differentiated into IgM-secreting plasma cells in these inflamed LN without any overt signs of proliferation, clonal expansion, or participation in GC responses (Fig. 6). Whether clonal expansion of B-1 cells occurred in tissues other than the MedLN cannot be formally excluded at this point. What argues against this is that there were no signs of increased B-1 cell numbers or B-1 cell–derived IgM-secreting cells in spleen, pleural and peritoneal cavities, or lung (unpublished data). Indeed, frequencies of B-1 cells seem to diminish in many of these tissues (Fig. 5 and not depicted), leading us to favor a model in which the regional accumulation of B-1 cells is caused by a redistribution rather than an expansion of these cells after infection (Fig. 8).

We previously demonstrated the importance of B-1 (and B-2) cell–derived IgM for survival from influenza virus infection (26) and showed the ability of natural B-1 cell–derived serum IgM to provide immune protection. More recently, Harada et al. (35) also demonstrated the potency of unmutated IgM in AID$^{-/-}$ mice to provide immune protection from influenza virus infection. Our studies here provide further evidence for the antiviral properties of natural IgM by showing their strong contribution to HI activity in the BLF (Fig. 3). Whether IgM might also contribute to immune protection by mechanisms other than direct binding and neutralization or complement-mediated virus inhibition, as indicated by recent studies by Carroll et al. (36), remains to be further evaluated.

If BCR-mediated activation does not drive B-1 cell responses to influenza, what signals induce their responses? Although it is only speculation at this point, given the strong evidence for innate signal-driven migration of B-1 cells (23, 32), we hypothesize that infection-induced proinflammatory signals, such as IL-1, IL-6, or TNF-α, might play a role in the recruitment of B-1 cells to the site of infection. These cytokines are induced locally as well as systemically after infection with influenza virus (not depicted) (37) and, thus, could induce B-1 cells to leave their sites of residence in the body cavities, and also possibly the spleen, and to accumulate in draining inflamed LN at the site of infection (Fig. 4 and Fig. 5). There is clear evidence for the regulation of B cell responses by proinflammatory cytokines. For example, IL-1 is required for local antiviral IgM responses to influenza virus infection (38), and IL-6 drives differentiation of B cells to plasma cells upon viral infection (39). Identification of signals that facilitate local B-1 cell activation will be important as a means to exploit the broadly reactive immunity provided by these cells.

An active participation of CD5$^+$ B-1a cells during influenza infection is in apparent contrast to recent findings by others, which showed that only CD5$^-$ B-1b cells actively responded to systemic infection with *B. hermsii*, whereas B-1a cells provided steady-state levels of natural antibacterial IgM (15, 16). Haas et al. (17) also demonstrated distinct functionalities of B-1a and B-1b cells in response to *S. pneumoniae* infection. Using mice that lacked either B-1a or B-1b cells because of the lack of or overexpression of CD19, respectively, they showed that only B-1b cells responded with PPS3-specific antibody production after immunization with PPS-3 and heat-killed bacteria and they conferred immunity after infectious challenge.

From these studies a "division of labor" between B-1a and B-1b cells was proposed, with B-1a cells providing passive protection via natural antibody production and B-1b cells responding actively to infection by providing antibodies and B cell memory (19). However, although B-1a cells did not provide PPS-3–specific responses (17), they generated strong responses to the cell wall membrane-component phosphocholine after immunization or infection (5, 6, 20–22).

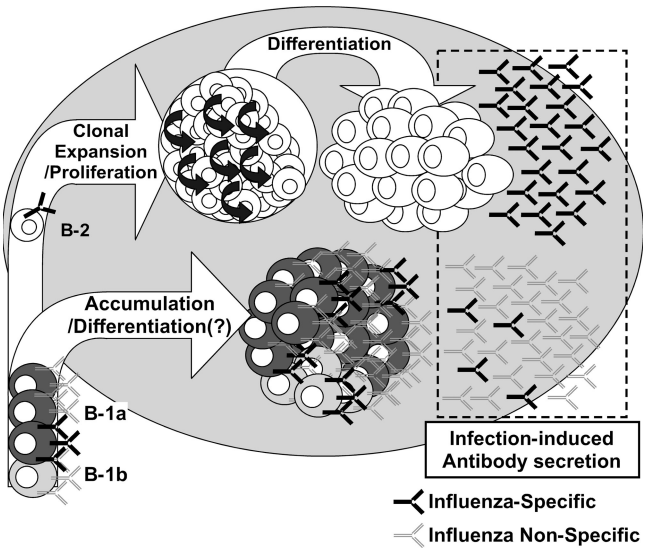

Figure 8. Working model of B-1a activation during influenza infection. After influenza virus infection, conventional (B-2) cell responses are characterized by infection-induced accumulation followed by vigorous antigen-specific clonal expansion/proliferation and differentiation into mainly isotype-switched virus-specific (black) antibody-secreting plasmablasts ($CD19^{lo}IgM^-IgD^-CD43^{hi}CD138^+$) in the regional LN at the site of infection. In contrast, B-1 cells (mostly B-1a) respond by similarly accumulating locally in the draining LN but failing to expand in response to antigen-specific signals. Instead, local inflammatory signals might drive their differentiation into short-lived ($CD5^+CD19^{hi}IgM^+CD43^+CD138^-$) IgM-secreting cells, thereby increasing local levels of poly-reactive virus-specific (black) and virus-nonspecific (gray) IgM at the site of infection. Without significant proliferation and/or antigen-specific clonal expansion, the B-1a cell–derived IgM response is not likely dependent on AID expression.

Collectively, our data and those of the *S. pneumoniae* model are not consistent with a mere passive role for B-1a cells. Instead, they indicate the need for strong (possibly innate) signals that induce B-1a cell responses, possibly via pattern-recognition receptor engagement of bacterial cell wall components in the case of *S. pneumoniae* and/or inflammatory-induced soluble stimuli such as cytokines, such as those induced in response to viral replication and virus-induced tissue destruction during influenza virus infection.

Systemic B-1a responses are not apparent after influenza virus infection (Fig. 2 and Fig. 4) (2) but are readily detectable in response to *S. pneumoniae* infection (21). This might be explained by the fact that *S. pneumoniae* induced a systemic infection in that study, whereas our studies with influenza induced a local respiratory tract–restricted infection. The ability of B-1 cells to respond in a localized tissue-restricted manner might have advantages for the host. B-1 cell–derived IgM is often poly-specific and reactive to self-antigens, although it is usually nonpathogenic and of low affinity. However, when inappropriately activated, B-1 cells can contribute to the development of antibody-mediated pathology as shown with transgenic mice expressing BCR specific to RBCs. B-1 cells developed normally in these mice and did not produce hemolytic anemia-causing IgM until stimulated with LPS (40). These data not only show that an innate signal alone is sufficient to cause B-1 cell activation and differentiation, they also indicate that B-1 cell activation must be tightly controlled to prevent systemic antibody-mediated autoimmunity. A sequestered local activation of B-1 cells in response to the vast majority of infections that we are exposed to at mucosal surfaces such as the respiratory and the gastrointestinal tract reduce the risk of autoimmune induction, while at the same time providing a rapid response system to reduce pathogen expansion during early infection. Because of the poly-specificity of the response, local increased production of B-1 cell–derived IgM might also reduce the risk of secondary infections that are common after influenza virus infection (41).

In summary, based on the data provided in this study, we propose a working model of B cell regulation to influenza (Fig. 8) in which mainly antigen-specific signals drive clonal expansion and differentiation of B-2 cells, while at the same time innate signals drive and target the movement and differentiation of B-1a cells to the site of infection. Consequently, "useful" poly-specific IgM responses are targeted to the site of infection, where they can confer immune protection against the primary infection as well as against potential superinfections by secondary infectious agents.

MATERIALS AND METHODS

Influenza virus and intranasal infection. Influenza A/Mem/71, a reassortant influenza virus strain carrying the hemagglutinin of A/Memphis/1/71 (H3) and the neuraminidase of A/Bellamy/42 (N1), was grown and harvested from the allantoic fluid of 10-d embryonated chicken eggs as previously described (42). Viral antigen was purified as previously described (43). Mice were anesthetized with isoflurane (MINRAD Inc.) and infected intranasally with a sublethal dose (12,000 PFU/mouse) of virus-containing allantoic fluid in 40 μl of sterile PBS.

Mice. 6–12-wk-old female and male C.B-17 (Taconic) and BALB/c (The Jackson Laboratory) mice, as well as pregnant female C.B-17 mice, were purchased and kept in microisolator cages under conventional housing conditions. Mice were used at 6–12 wk of age or used to generate chimeras according to protocols approved by the University of California, Davis Animal Use and Care Committee. Ig allotype chimeras were generated as previously described (12, 44) to distinguish B-1 and B-2 cells and the IgM they secrete with help of allotype- and isotype-specific mAb. In brief, newborn C.B-17 mice (Igh-b) received 0.1 mg of anti-IgMb (AF6-78.2.5) antibody i.p., purified by Hi-Trap Affinity Protein G Column (GE Healthcare) from serum-free tissue culture supernatants to deplete host (Igh-b) B cells. Antibody treatment was continued for 6 wk, giving biweekly injections of 0.2 mg for a total of 2 mg/mouse of anti-IgMb. 2 d after birth, mice also received 3–5 × 10^6 PerC from 2-mo-old congenic BALB/c (Igh-a) mice as source for allotype disparate B-1 cells. Allotype chimeras were held for at least two additional months after cessation of antibody treatment before being used in experiments.

Irradiation Ig allotype chimeras were established by reconstituting lethally irradiated C.B-17 (Igh-b; n = 4/group) mice (650 rad of full body irradiation) with total PerC (2 × 10^6 cells/mouse) or FACS-purified B-1a (2.2 × 10^6 cells/mouse) and B-1b cells (5.2 × 10^5 cells/mouse) from BALB/c mice (Igh-a) together with 2 × 10^6 BM cells from C.B-17 mice. We transferred the highest number of B-1b cells into each mouse that we could obtain from FACS purification of PerC pooled from 24 mice. B-1a cells were transferred at numbers that reflected their relative proportion in the PerC compared with B-1b cells (ratio of just over 4:1) as established by FACS. Irradiated Ig allotype chimeras were rested for 4–6 wk before the onset of experiments. Chimerism was confirmed by ELISA, which revealed the presence of total and virus IgM in the serum of noninfected reconstituted mice. The Animal Use and Care Committee of the University of California, Davis approved all procedures and experiments involving mice.

BrdU incorporation. For BrdU incorporation studies, groups of BALB/c mice (n = 4) either infected with A/Mem/71 or mock infected using PBS received BrdU (1 mg/100 μl PBS) i.p. and additional BrdU ad libitum in the drinking water (1 mg/100 ml) on day 6 after infection. BrdU incorporation was analyzed 24 h later, i.e., on day 7 after infection.

ELISPOT. To quantify total and virus-specific B-1 and B-2 cell–derived IgM producers, 96-well plates (Multi-Screen HA Filtration; Millipore) were coated with 5 μg/ml of anti-IgM (mAb 331, not allotype-specific) or 1,000 HAU/ml of purified A/Mem/71 as previously described (43). After blocking with PBS with 4% BSA, serial dilutions of single cells from various tissues were incubated overnight in culture medium (RPMI 1640, 2 mM L-glutamine, 100 μg/ml of penicillin and streptomycin, 10% heat inactivated FCS, and 50 μM 2-ME) at 37°C with 5% CO_2. Binding was revealed with in house–generated biotinylated allotype-specific anti-IgM (DS-1.1 for IgM^a and AF6-78.2.5 for IgM^b) followed by SA-HRP (Vector Laboratories) and 3-amino-9-ethylcarbazole (Sigma-Aldrich). Spots were counted with the help of a stereomicroscope (Stemi 2000-C; Carl Zeiss, Inc.). Data are expressed as the number of total and virus-specific IgM-secreting cells per input cells.

ELISA. Total and virus-specific serum IgM levels were determined by ELISA as described previously (43). In brief, 5 μg/ml of anti-IgM (331) antibody and 1,000 HAU/ml of purified A/Mem/71 were coated onto 96-well plates (Maxisorb; Thermo Fisher Scientific). After blocking nonspecific protein binding, serially diluted serum was added to plates. Binding was revealed with biotinylated allotype-specific anti-IgM antibodies as outlined under ELISPOT. Purified myeloma IgM from HPC-76 (IgM^a) and CBPC-112 (IgM^b), respectively, served as standards. Arbitrary units of A/Mem/71-specific IgM titers, defined as U/ml, were determined by comparison to hyperimmune sera from BALB/c (Igh-a) and C.B-17 (Igh-b) mice. Half-maximal binding of that serum at a predetermined dilution was set as 100 U.

BLF. BLF was taken by instilling 1 ml of sterile-filtered PBS through the trachea into the lung airways and aspirating it with help of a syringe.

Cell-free supernatant was stored at −80°C until analyzed. Total protein levels in BLF were determined by Bradfort protein assay (Bio-Rad Laboratories). Antibody concentrations in BLF were normalized to total protein concentrations and expressed as IgM/protein (in micrograms/milligram) and virus-specific IgM/protein (in units/milligram).

HI assay. HI assay was performed with BLF from mice before and at 7 d after infection and before and after removal of IgM. IgM was removed from BLF by anti-IgM (mAb 331) column affinity chromatography with columns generated according to the manufacturer's instructions (AminoLink Coupling Gel; Thermo Fisher Scientific). Micro-HI assay was done as previously reported (45). In brief, 25 µl of serially twofold-diluted BLF was incubated with 4 HAU A/Mem/71 in 25 µl using a 96-well plate and incubated at room temperature for 30 min. 25 µl of fresh chicken RBCs (Hemostat Laboratories) at 1% (volume/volume) in PBS was added to each well and incubated at room temperature for 1 h. Hemagglutination was determined by eye. HI titers were determined as the last reciprocal sample dilutions that fully inhibited influenza virus hemagglutination.

Flow cytometry. Single cell suspensions from PerC, spleen, PLN, and MedLN were stained exactly as outlined previously (43) with the following antibody conjugates (in-house generated unless otherwise noted) at predetermined optimal concentrations after Fc receptor block: CD3-Cy5-PE (145-2C11), CD4-Cy5-PE (GK1.5; eBioscience); CD19-Cy5.5-allophycocyanin (6D5; Invitrogen); CD43-PE (S7), CD5-PE (53–7.8), and CD138-PE (BD); Streptavidin-QDot605A (Invitrogen); and CD8-Cy5-PE (53.6.7), F4/80-Cy5-PE (F4/80), IgD-Cy7-PE (11–26), and IgD^a-Cy7-PE (AMS-9.1), IgM allophycocyanin (331), and IgM^b allophycocyanin (AF6-68.2.5), IgM^a-Biotin (DS-1.1), CD24-Cy5.5-PE (30F1.2), and CD38-FITC (clone 90). Propodium iodide was added to stained cells at 1 µg/ml to discriminate dead cells. Intranuclear BrdU staining was identified as described previously (46).

For FACS purification of B-1a and B-1b cells, cell populations were isolated from PerC of BALB/c (Igh-a) mice and stained as described previously (43) with CD5-biotin (53–7.8), CD11b-Cy7-PE (Mac1), CD19-APC (ID3); CD23-FITC (B3B4; BD); and Streptavidin-QDot605A (Invitrogen). Data acquisition and sorting were done using a FACSAria (BD) equipped with lasers and optics for 13-color data acquisition (46). Data analysis was done using FlowJo software (gift of A. Treestar, Tree Star Inc.).

Statistical analysis. Statistical analysis was done using either the two-tailed Student's *t* test or the nonparametric one-way ANOVA test. Data were regarded as statistically significant at $P < 0.05$.

We thank Virginia Doucett for support in establishing Ig allotype chimeras, Abigail Spinner for help and advice in operating the FACSAria, and Dr. Michael McChesney for helpful comments and suggestions on the manuscript.

Theses studies were supported by grant AI051354 from the National Institutes of Health/NIAID to N. Baumgarth and partial tuition support to Y.S. Choi from the Graduate Group in Immunology at the University of California, Davis.

The authors have no conflicting financial interests.

Submitted: 6 May 2008
Accepted: 17 November 2008

REFERENCES

1. Avrameas, S. 1991. Natural autoantibodies: from 'horror autotoxicus' to 'gnothi seauton'. *Immunol. Today*. 12:154–159.
2. Baumgarth, N., O.C. Herman, G.C. Jager, L.A. Herzenberg, and L.A. Herzenberg. 1999. Innate and acquired humoral immunities to influenza virus are provided by distinct arms of the immune system. *Proc. Natl. Acad. Sci. USA*. 96:2250–2255.
3. Casali, P., and E.W. Schettino. 1996. Structure and function of natural antibodies. *Curr. Top. Microbiol. Immunol*. 210:167–179.
4. Coutinho, A., M.D. Kazatchkine, and S. Avrameas. 1995. Natural autoantibodies. *Curr. Opin. Immunol*. 7:812–818.
5. Briles, D.E., M. Nahm, K. Schroer, J. Davie, P. Baker, J. Kearney, and R. Barletta. 1981. Antiphosphocholine antibodies found in normal mouse serum are protective against intravenous infection with type 3 *Streptococcus pneumoniae*. *J. Exp. Med*. 153:694–705.
6. Briles, D.E., C. Forman, S. Hudak, and J.L. Claflin. 1982. Anti-phosphorylcholine antibodies of the T15 idiotype are optimally protective against *Streptococcus pneumoniae*. *J. Exp. Med*. 156:1177–1185.
7. O'Brien, A.D., I. Scher, G.G. Campbell, R.P. MacDermott, and S.B. Formal. 1979. Susceptibility of CBA/N mice to infection with Salmonella typhimurium: Influence of the X-linked gene controlling B lymphocyte function. *J. Immunol*. 123:720–724.
8. Ochsenbein, A.F., T. Fehr, C. Lutz, M. Suter, F. Brombacher, H. Hengartner, and R.H. Zinkernagel. 1999. Control of early viral and bacterial distribution and disease by natural antibodies. *Science*. 286: 2156–2158.
9. Stall, A.M., S. Adams, L.A. Herzenberg, and A.B. Kantor. 1992. Characteristics and development of the murine B-1b (Ly-1 B sister) cell population. *Ann. N. Y. Acad. Sci*. 651:33–43.
10. Montecino-Rodriguez, E., H. Leathers, and K. Dorshkind. 2006. Identification of a B-1 B cell-specified progenitor. *Nat. Immunol*. 7: 293–301.
11. Kantor, A.B., A.M. Stall, S. Adams, L.A. Herzenberg, and L.A. Herzenberg. 1992. Differential development of progenitor activity for three B-cell lineage. *Proc. Natl. Acad. Sci. USA*. 89:3320–3324.
12. Lalor, P.A., L.A. Herzenberg, S. Adams, and A.M. Stall. 1989. Feedback regulation of murine Ly-1 B cell development. *Eur. J. Immunol*. 19:507–513.
13. Bikah, G., J. Carey, J.R. Ciallella, A. Tarakhovsky, and S. Bondada. 1996. CD5-mediated negative regulation of antigen receptor-induced growth signals in B-1 B cells. *Science*. 274:1906–1909.
14. Morris, D.L., and T.L. Rothstein. 1993. Abnormal transcription factor induction through the surface immunoglobulin M receptor of B-1 lymphocytes. *J. Exp. Med*. 177:857–861.
15. Alugupalli, K.R., R.M. Gerstein, J. Chen, E. Szomolanyi-Tsuda, R.T. Woodland, and J.M. Leong. 2003. The resolution of relapsing fever Borreliosis requires IgM and is concurrent with expansion of B1b lymphocytes. *J. Immunol*. 170:3819–3827.
16. Alugupalli, K.R., J.M. Leong, R.T. Woodland, M. Muramatsu, T. Honjo, and R.M. Gerstein. 2004. B1b lymphocytes confer T cell-independent long-lasting immunity. *Immunity*. 21:379–390.
17. Haas, K.M., J.C. Poe, D.A. Steeber, and T.F. Tedder. 2005. B-1a and B-1b cells exhibit distinct developmental requirements and have unique functional roles in innate and adaptive immunity to *Streptococcus pneumoniae*. *Immunity*. 23:7–18.
18. Hsu, M.C., K.M. Toellner, C.G. Vinuesa, and I.C.M. MacLennan. 2006. B cell clones that sustain long-term plasmablast growth in T-independent extrafollicular antibody responses. *Proc. Natl. Acad. Sci. USA*. 103:5905–5910.
19. Alugupalli, K.R., and R.M. Gerstein. 2005. Divide and conquer: division of labor by B-1 B cells. *Immunity*. 23:1–2.
20. Claflin, J.L., S. Hudak, and A. Maddalena. 1981. Anti-phosphocholine hybridoma antibodies I. Direct evidence for three distinct families of antibodies in the murine response. *J. Exp. Med*. 153:352–364.
21. Masmoudi, H., T. Mota-Santos, F. Huetz, A. Coutinho, and P.A. Cazenave. 1990. All T15 Id-positive antibodies (but not the majority of VHT15+ antibodies) are produced by peritoneal CD5+ B lymphocytes. *Int. Immunol*. 2:515–520.
22. Wallick, S., J.L. Claflin, and D.E. Briles. 1983. Resistance to *Streptococcus pneumoniae* is induced by a phosphocholine-protein conjugate. *J. Immunol*. 130:2871–2875.
23. Yang, Y., J.W. Tung, E.E.B. Ghosn, L.A. Herzenberg, and L.A. Herzenberg. 2007. Division and differentiation of natural antibody-producing cells in mouse spleen. *Proc. Natl. Acad. Sci. USA*. 104:4542–4546.
24. Brandtzaeg, P. 1989. Overview of the mucosal immune system. *Curr. Top. Microbiol. Immunol*. 146:13–24.
25. Gerhard, W., K. Mozdzanowska, M. Furchner, G. Washko, and K. Maiese. 1997. Role of the B-cell response in recovery of mice from primary influenza virus infection. *Immunol. Rev*. 159:95–103.

26. Baumgarth, N., O.C. Herman, G.C. Jager, L.E. Brown, L.A. Herzenberg, and J. Chen. 2000. B-1 and B-2 cell–derived immunoglobulin M antibodies are nonredundant components of the protective response to influenza virus infection. *J. Exp. Med.* 192:271–280.
27. Savitsky, D., and K. Calame. 2006. B-1 B lymphocytes require Blimp-1 for immunoglobulin secretion. *J. Exp. Med.* 203:2305–2314.
28. Baumgarth, N. 2004. B cell immunotyping. *Methods Cell Biol.* 75: 643–662.
29. Stall, A.M., S.M. Wells, and K.P. Lam. 1996. B-1 cells: unique origins and functions. *Semin. Immunol.* 8:45–59.
30. Ohdan, H., K.G. Swenson, H.S.K. Gray, Y.-G. Yang, Y. Xu, A.D. Thall, and M. Sykes. 2000. Mac-1-negative B-1b phenotype of natural antibody-producing cells, including those responding to Galα1,3Gal epitopes in α1,3-galactosyltransferase-deficient mice. *J. Immunol.* 165:5518–5529.
31. Shinall, S.M., M. Gonzalez-Fernandez, R.J. Noelle, and T.J. Waldschmidt. 2000. Identification of murine germinal center B cell subsets defined by the expression of surface isotypes and differentiation antigens. *J. Immunol.* 164:5729–5738.
32. Ha, S.A., M. Tsuji, K. Suzuki, B. Meek, N. Yasuda, T. Kaisho, and S. Fagarasan. 2006. Regulation of B1 cell migration by signals through toll-like receptors. *J. Exp. Med.* 203:2541–2550.
33. Tarakhovsky, A., S.B. Kanner, J. Hombach, J.A. Ledbetter, W. Muller, N. Killeen, and K. Rajewsky. 1995. A role for CD5 in TCR-mediated signal transduction and thymocyte selection. *Science.* 269:535–537.
34. Goodnow, C.C., J. Crosbie, S. Adelstein, T.B. Laboie, S.J. Smith-Gill, R.A. Brink, H. Pritchard-Briscoe, J.S. Wotherspoon, R.H. Loblay, K. Raphael, et al. 1988. Altered immunoglobulin expression and functional silencing of self-reactive B lymphocytes in transgenic mice. *Nature.* 334: 676–682.
35. Harada, Y., M. Muramatsu, T. Shibata, T. Honjo, and K. Kuroda. 2003. Unmutated immunoglobulin M can protect mice from death by influenza virus infection. *J. Exp. Med.* 197:1779–1785.
36. Jayasekera, J.P., E.A. Moseman, and M.C. Carroll. 2007. Natural antibody and complement mediate neutralization of influenza virus in the absence of prior immunity. *J. Virol.* 81:3487–3494.
37. Brydon, E.W.A., S.J. Morris, and C. Sweet. 2005. Role of apoptosis and cytokines in influenza virus morbidity. *FEMS Microbiol. Rev.* 29:837–850.
38. Schmitz, N., M. Kurrer, M.F. Bachmann, and M. Kopf. 2005. Interleukin-1 is responsible for acute lung immunopathology but increases survival of respiratory influenza virus infection. *J. Virol.* 79:6441–6448.
39. Jego, G., A.K. Palucka, J.P. Blanck, C. Chalouni, C. Pascual, and J. Banchereau. 2003. Plasmacytoid dendritic cells induce plasma cell differentiation through type I interferon and interleukine 6. *Immunity.* 19: 225–234.
40. Murakami, M., T. Tsubata, R. Shinkura, S. Nisitani, M. Okamoto, H. Yoshioka, T. Usui, S. Miyawaki, and T. Honjo. 1994. Oral administration of lipopolysaccharides activates B-1 cels in peritoneal cavity and lamina propria of the gut and induces autoimmune symptoms in an autoantibody transgenic mouse. *J. Exp. Med.* 180:111–121.
41. Hayashi, K., S. Kadowaki, M. Takei, and H. Fukuda. 2006. Efficacy of quinolones against secondary pneumococcal pneumonia after influenza virus infection in mice. *Antimicrob. Agents Chemother.* 50:748–751.
42. Baumgarth, N., L. Brown, D. Jackson, and A. Kelso. 1994. Novel features of the respiratory tract T-cell response to influenza virus infection: lung T cells increase expression of gamma interferon mRNA in vivo and maintaining high levels of mRNA expression for interleukin-5 (IL-5) and IL-10. *J. Virol.* 68:7575–7581.
43. Doucett, V.P., W. Gerhard, K. Owler, D. Curry, L. Brown, and N. Baumgarth. 2005. Enumeration and characterization of virus-specific B cells by multicolor flow cytometry. *J. Immunol. Methods.* 303:40–52.
44. Forster, I., and K. Rajewsky. 1987. Expansion and functional activity of Ly-1+ B cells upon transfer of peritoneal cells into allotype-congenic, newborn mice. *Eur. J. Immunol.* 17:521–528.
45. Bachmann, M.F., B. Ecabert, and M. Kopf. 1999. Influenza virus: a novel method to assess viral and neutralizing antibody titers in vitro. *J. Immunol. Methods.* 225:105–111.
46. Rothaeusler, K., and N. Baumgarth. 2006. Evaluation of intranuclear BrdU detection procedures for use in multicolor flow cytometry. *Cytometry A.* 69:249–259.